



CRYSTAL GROWTH, EXPERIMENTAL, AND THEORETICAL INVESTIGATION OF ORGANIC NLO MATERIAL N, N DIMETHYL-4 NITRO ANILINE

Bhuvanewari G¹, Prabavathi N^{2*} and Guru Prasad L³

¹Department of Physics, Muthayammal college of Arts and Science, Rasipuram,

²Department of Physics, Sri Sarada College for Women (Autonomous), Salem-636 016,

³Department of Science & Humanities, M.Kumaraswamy college of Engineering, Karur

ARTICLE INFO

Article History:

Received 6th September, 2018

Received in revised form 15th October, 2018

Accepted 12th October, 2018

Published online 28th December, 2018

Key words:

Powder and single crystal XRD, UV-Vis, TGDTA, SHG, Hyperpolarisability,

ABSTRACT

The adequate size of N,N Dimethyl 4 Nitroaniline single crystal have been grown by solution growth slow evaporation technique at room temperature by using methanol as a solvent. The Vibrational and electronic properties of the grown crystal was carried out by FTIR, FT-Raman and UV -Vis analysis respectively and also the Density Functional theory (DFT) method, using B3LYP (6-311++G(d,p)) which gives the useful information about vibrational assignments of the grown crystal. The Powder and single crystal XRD reveals that the crystalline structure of the grown material. Hyperpolarizability and electric dipole moment values have been calculated theoretically by using Gaussian 09 Package. TGDTA study has been used to investigate the thermal stability of the grown crystal. By using the Kurtz and Perry method the second harmonic frequency conversion process was examined.

Copyright©2018 Bhuvanewari G., Prabavathi N and Guru Prasad L. This is an open access article distributed under the Creative Commons Attribution License, which permits unrestricted use, distribution, and reproduction in any medium, provided the original work is properly cited.

INTRODUCTION

Some ortho, meta, and Para disubstituted benzene derivatives possessing high non linear properties [1]. Particularly p-nitro aniline, m- nitro aniline and some other related structure exhibits large second harmonic non- linear property. The π -electron charge transfer property of the compound provides high hyperpolarisability [2, 3]. The second order NLO organic materials that contain large hyperpolarisability in non-centrosymmetric packing system is suitable for opto electronic devices [4,5]. Due to these reasons, the compound N, N-dimethyl-4-nitroaniline was chosen for the present study. In this paper the vibrational assignments, Thermal, optical, and NLO property of the grown crystal. Some theoretical values of hyperpolarisability, NBO (Natural bond analysis), and HOMO-LUMO analysis (Higher occupied molecular orbital and lower unoccupied orbital) are determined by using Gaussian 98W package. The donor -acceptor substituted benzene compounds are specially contribute the area of NLO material because they are very good model for crystalline hyperpolarisabilities[6,7]which can be able to understand from the computational approaches. The fruitful explanation of the molecular hyperpolarisability has been developed in the publication[8]

MATERIAL AND METHODS

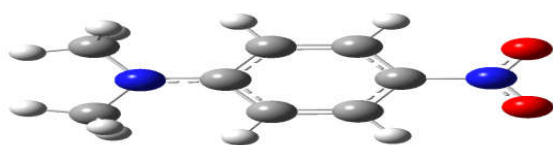
The single crystal of DMNA was prepared from the slow evaporated solution growth technique. The commercially available organic compound under investigation namely N,N Dimethyl 4 Nitroaniline (DMNA) was purchased from Alfa aesar (98%). The saturated solution of title compound is prepared from methanol is used as a solvent. Then it was filtered by Whatmann filter paper to remove the unwanted suspended materials. This purified solution was tightly covered by a perforated polythene sheet and kept to allow the evaporation. The good quality crystal was grown after 4 weeks and the photographic image is shown in fig.1 (a)



(a)

***Corresponding author: Prabavathi N**

Department of Physics, Sri Sarada College for Women,
Salem-636 016,



(b)

Fig 1 (b) Photograph of as grown crystal and Optimized structure of DMNA

RESULT AND DISCUSSION

Powder XRD and Single crystal XRD

The powder XRD Pattern of the DMNA crystal has been studied by using SHIMADZU XRD 6000 X-ray diffractometer is shown in Fig.2. From the XRD pattern analysis, the sharp intense peak helps to prove the good crystalline nature of the grown crystal. Lattice cell parameter was also been determined and the values are good agreement with the reported values (JCPDS File No-25-1766). The single crystal XRD using Bruker AXS Kappa APEX II CCD diffractometer and the calculated values are tabulated. The DMNA crystal system belongs to the monoclinic with noncentrosymmetric space group of P_{21} . The main advantage of noncentrosymmetric space group evidences the frequency conversion process and also the crystal is useful for the fabrication of opto electronic devices.

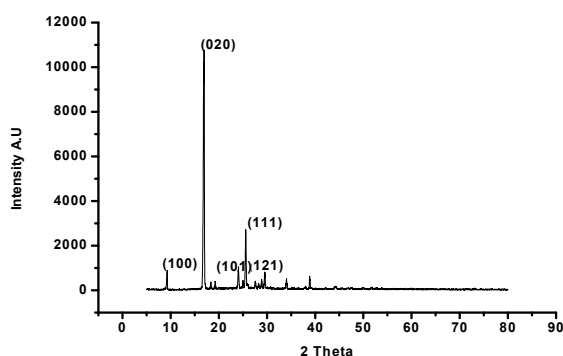


Fig 2 Powder XRD Pattern for DMNA

Table 1 Cell parameters of DMNA

	As grown crystal of DMNA	Reported values[JCPDS File No-25-1766]
Molecular formula	$C_8H_{10}N_2O_2$	$C_8H_{10}N_2O_2$
Molecular weight	166.18	166.18
Crystal system	Monoclinic, P_{21}	Monoclinic, P_{21}
Unit cell parameters	$a = 3.916(3) \text{ \AA}$ $b = 10.618(11) \text{ \AA}$ $c = 9.746(8) \text{ \AA}$	$a = 3.974 \text{ \AA}$ $b = 10.574 \text{ \AA}$ $c = 9.734 \text{ \AA}$
Volume	$409.8(4) \text{ \AA}^3$	408.92 \AA^3

Computational details

The quantum chemical calculations of DMNA compound are achieved by using Gaussian 09 program B3LYP /6-311++G(d,p) basis set. [9]. The optimized geometries corresponding to the minimum on the potential energy surface are obtained by finding self-consistent field equation iteratively. Harmonic vibrational wave numbers are determined by using analytic second order derivatives and additionally ensure the convergence to minima on the potential energy surface and to evaluate the zero-point vibrational

energy [10]. The natural bonding orbital's (NBO) calculations [11] are performed using NBO 3.1 program in order to understand various second-order interactions between the filled orbital's of one subsystem and vacant orbital's of another subsystem, which is a measure of the intermolecular delocalization or hyper conjugation. The hyper conjugative interaction energy was deduced from the second-order perturbation approach[12].

Hyperpolarizability

The static initial hyperpolarizability (β_0) of DMNA is calculated based on the finite-field approach and the calculated values are shown in Table 2. In the presence of an applied electric field, the ene0rgy of a system is a function of the electric field. First hyperpolarizability is a third rank tensor that can be described by a $3 \times 3 \times 3$ matrix. Due to the use of Kleinman symmetry the 27 components of the 3D matrix can be reduced to ten components [13]. It can be given in the lower part of the $3 \times 3 \times 3$ matrices is tetrahedral format. The components of β are defined as the coefficients in the Taylor series of expansion of energy in the external electric field. The total static dipole moment μ , the mean polarizability α_0 , the anisotropy of the polarizability $\Delta\alpha$ and the static first hyperpolarizability β_0 , using the x, y, z components are defined as given in the literature [14]. Since the values of hyperpolarizability (β) of the Gaussian 09 output are reported in atomic units (a.u.), the calculated values have been converted into electrostatic units (esu).

Table 2 The First order hyperpolarizability of DMNA

β components	B3LYP/6-311++G(d,p)
β_{xxx}	-2891.1344
β_{xxy}	0.0118661
β_{xyy}	257.69672
β_{yyy}	-0.0084963
β_{xxx}	2.7631458
β_{xyz}	0.0175522
β_{yyz}	2.1918082
β_{xzz}	103.3858862
β_{yzz}	-0.0028678
β_{zzz}	5.7749644
β_{tot}	$2.5301 \times 10^{-30} \text{ e.s.u}$

The calculated β components $\sim (-2\omega, \omega, \omega)$ in 10^{-30} esu The determined β value of DMNA is 2.5301×10^{-30} e.s.u which is nearly 13 times greater than urea(0.1947×10^{-30} e.s.u).

NBO analysis

The natural bond orbital (NBO) analysis gives a detailed explanation of the structure of a conformer by a set of localized bond, antibonds and Rydberg extra valence orbitals. Stabilizing interactions between filled and unoccupied orbitals and destabilizing interactions between filled orbitals can also be obtained from this analysis [15, 16]. NBO analysis is used to find the interaction between the bond orbitals, electron delocalization, bond bending effect, intramolecular charge transfer (ICT) and identification of hydrogen bonding. The NBO's obtained in this concept correspond to the widely used lewis picture, in which two-center bonds and lone pairs are localized [17]. The larger the E (2) value, the high intensive is the interaction between electron donors and acceptors, i.e. the more electrons donating tendency from electron donors to acceptors and greater the extent of conjugation of the whole system. The intramolecular hyper conjugative interactions are formed by the orbital overlap between $[\sigma$ and π (C-C, C-N and

C-H) and σ^* and π^* (C-C, C-N and C-H)] bond orbitals which results Intermolecular Charge Transfer (ICT) causing stabilization of the system. These interactions are observed as increase in electron density (ED) in C-C, C-N and C-H antibonding orbital that weakens the respective bonds [18]. A large number of stabilizing orbital interactions are calculated in DMNA and they are listed in Tables 3. The maximum stabilization energy arises for $C_2-C_3(\pi)$ to $C_4 - C_5(\pi^*)$, $C_4-C_5(\pi)$ to $C_6-C_7(\pi^*)$, and $C_4-C_5(\pi)$ to $N_8-O_9(\pi^*)$ with energy of about 29.21, 23.90, and 23.79 kJ/mol respectively. The charge transferred value from DMNA lone pair nitrogen LP(1)N₁₁ shows the stabilization energy 49.08 kJ/mol.

Table 3 The second order perturbation energies E(2)(Kj/mol) corresponding to the charge transfer between donor - acceptor in DMNA

NBO(i)	TYPE	E _D /e	NBO(j)	TYPE	E _D /e	E(2) (Kj/mol)	E _i -E _j (a.u)	F(i,j) (a.u)
C ₂ -C ₃	π	1.58525	C ₄ -C ₅	π^*	0.42555	29.21	0.28	0.081
			C ₆ -C ₇	π^*	0.29566	13.74	0.28	0.057
C ₄ -C ₅	π	1.64000	C ₂ -C ₃	π^*	0.43768	15.17	0.28	0.059
			C ₆ -C ₇	π^*	0.29566	23.90	0.29	0.075
C ₆ -C ₇	π	1.72493	N ₈ -O ₉	π^*	0.65253	23.79	0.14	0.062
			C ₂ -C ₃	π^*	0.43768	21.82	0.28	0.072
N ₁	LP(1)	1.69465	C ₄ -C ₅	π^*	0.42555	14.17	0.28	0.060
			C ₂ -C ₃	π^*	0.43768	49.08	0.27	0.106
O ₉	LP(2)	1.90249	C ₅ -N ₈	σ^*	0.09650	11.22	0.59	0.072
			N ₈ -O ₁₀	σ^*	0.05504	18.91	0.72	0.105
O ₁₀	LP(2)	1.90254	C ₅ -N ₈	σ^*	0.09650	11.21	0.59	0.072
			N ₈ -O ₉	σ^*	0.05501	18.90	0.72	0.105

E(2) means energy of hyperconjugative interaction (stabilization energy)
E_i - E_j means the energy difference between donor and acceptor i and j NBO orbitals

F(i,j) is the Fock matrix element between i and j NBO orbitals

FTIR and FT-Raman

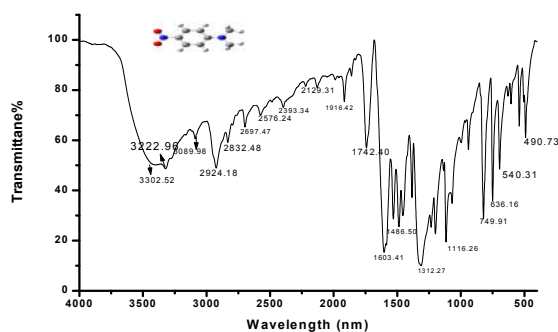


Fig 3 FTIR

4 DMNA molecules consist of 22 atoms which gives 60 normal modes of vibrational and 60 degrees of freedom. The FTIR spectrum has been observed in the range of 400- 4000 cm^{-1} using IFS Bruker FT IR Spectrometer and FT-Raman spectrum has been illustrated in the range of 400- 4000 cm^{-1} using Bruker RFS 27 Spectrometer. The spectrum pattern is shown in Fig. 3 and 4. Theoretically the experimental wave numbers are smaller than the calculated values. This discrepancy can be corrected by using the empirical scaling procedure which is excellently to agree the experimental and theoretical frequencies. For the B3LYP/6-31G (d,p) level of scaling factor of 0.956 has been consistently applied to the computed wave numbers. The calculated and experimental results were compared and it is found that there is an excellent

agreement between them at the DFT level which are given in Table 2

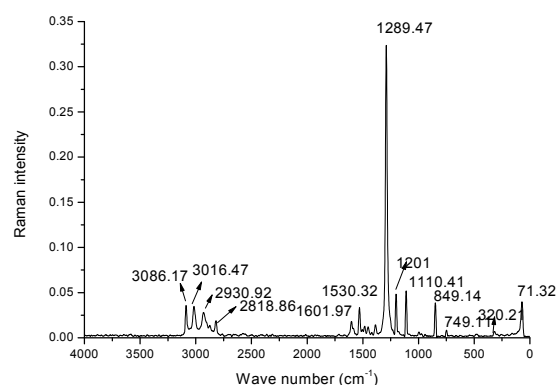


Fig 4 FT-Raman

C-H Vibrations

In general C-H vibrations are traced in the region between 3000 -3100 cm^{-1} [19]. The present theoretical investigation found that ten C-H stretching vibrations are identified at 3094.714, 3093.629, 3082.013, 3080.765, 3015.763, 3002.698, 2922.672, 2921.866, 2884.474 and 2878.176 cm^{-1} with contribution of average % of PED is about 97%.

The strong intensity bands are occur in the region between 1000-1300 cm^{-1} are characterized by C-H inplane bending vibrations [20]. The in plane C-H bending vibrations are occur at 1116, 1136, 1200 and 1273 cm^{-1} in FTIR. These observed vibrations are identical with theoretical observations at 1099, 1146, 1214 and 1286 cm^{-1} and they are found to be mixed with C-C stretching vibrations. Among the four vibrations only three are present in both FTIR and Raman spectra.

C-C Vibrations

The ring vibrations were observed in the region between 915-1591 cm^{-1} and 941-1626 cm^{-1} experimentally and theoretically [21]. In DMNA theoretically there are seven C-C stretching vibrations are identified. Out of seven, only four vibration are present in FTIR at 1116, 1200, 1584 and 1603 cm^{-1} . For the same vibration three peaks are identified at 1110, 1201 and 1601 cm^{-1} in FT-Raman. Thus the experimental values more related with theoretical data.

C-N Vibrations

Silverstein *et al.* [22] observed that the C-N vibration are identified in the region 1382-1266 cm^{-1} . Aromatic amines strongly absorbed in the region about 1300 cm^{-1} due to C=N stretching vibrations. In both FTIR and FT-Raman vibrations are traced at 1384 and 1386 cm^{-1} . These assignments are also in good agreement with the theoretical value.

N-O Vibrations

Aromatic nitro compounds have produced the strong peak in the region of 1570-1485 cm^{-1} and 1370-1320 cm^{-1} [23] which exhibits due to the symmetric and asymmetric stretching vibration of Nitro group. The strong peak observed at 1486 cm^{-1} in FTIR and 1483 cm^{-1} in FT-Raman are identified for NO₂ symmetric stretching mode. The symmetric stretching vibration are assigned at 1486 cm^{-1} which are closely related with theoretical calculation.

Table 2 Observed and B3LYP/6-31G* level calculated vibrational frequency assignments of 4DMNA

S.No	Observed frequencies (cm ⁻¹)		Calculated frequencies(cm ⁻¹) with B3LYP/6-31++G*level				PED(%)
	Infrared	Raman	Unscaled	Scaled	IR	Raman	
1	3222.52	-	3223.66	3094.714	8.2434	193.2950	CH _{ss} (99)
2	3202.96	-	3222.53	3093.629	0.924	0.3686	CH _{ss} (99)
3	3089.58	3086.91	3210.43	3082.013	4.2574	66.9118	CH _{ss} (99)
4	-	-	3209.13	3080.765	1.1368	2.2219	CH _{ss} (99)
5	-	-	3141.42	3015.763	30.3720	182.9398	CH _{ss} (94)
6	-	-	3127.81	3002.698	1.761	1.8492	CH _{ss} (93)
7	2924.18	2930.92	3044.45	2922.672	65.2685	49.8076	CH _{ss} (100)
8	-	-	3043.61	2921.866	0.1276	158.4793	CH _{ss} (100)
9	-	-	3004.66	2884.474	58.0422	345.6136	CH _{ss} (94)
10	-	2818.86	2998.10	2878.176	83.2536	75.7455	CH _{ss} (93)
11	1603.41	1601.79	1643.14	1577.414	331.387	159.3908	CC _{ss} (57), bHCC(19),bCCC(10)
12	1584.47	-	1620.38	1555.565	101.5339	2.0477	CC _{ss} (49), bCNC(13),
13	1530.95	1530.32	1550.84	1488.806	171.7666	35.2727	NC _{ss} (11), bHCC(45)
14	1486.50	1483.07	1548.01	1486.09	183.438	20.4869	ON _{ss} (69)
15	1459.37	1452.68	1526.16	1465.114	6.9953	24.0923	bHCH(58),HCNC Tring(21)
16	-	-	1514.35	1453.776	1.1571	2.4433	bHCH(60),HCNC Tring(20)
17	-	-	1495.12	1435.315	17.2237	21.0515	bHCH(65),HCNC Tring(19), HCNC Tring(10)
18	-	-	1487.82	1428.307	20.4140	7.8612	bHCC(82)
19	-	-	1486.19	1426.742	0.0223	7.4384	bHCH(62),HCNC Tring(24)
20	-	-	1467.90	1409.184	9.2487	1.0250	CC _{ss} (43), bHCC(21), bHCH(14)
21	-	-	1449.07	1391.107	3.0085	13.6599	bHCH(80)
22	1384.12	1386.60	1395.16	1339.354	29.1447	29.1439	NC _{ss} (41), bHCC(18) HCNC Tring(10)
23	1312.27	-	1374.14	1319.174	6.9024	0.8283	bCNC(14) NC _{ss} (14)
24	-	-	1344.95	1291.152	1085.6039	1057.6836	ON _{ss} (76), bONO(10) HCNC Tring(10)
25	1273.72	1289.49	1339.73	1286.141	1.8094	0.2153	bHCC(73)
26	1200.21	1201.32	1265.25	1214.64	26.8192	7.7804	NC _{ss} (39), CC _{ss} (11), HCNC Tring(12)
27	-	-	1219.79	1170.998	41.8109	4.0215	bHCC(57), CC _{ss} (12)
28	1136.26	-	1193.92	1146.163	7.7538	10.2235	bHCH(13) HCNC Tring(47)
29	1116.26	1110.90	1144.85	1099.056	5.7200	0.0021	bHCC(64) CC _{ss} (25)
30	-	-	1136.99	1091.51	0.1223	0.5773	bHCH(21),HCNC Tring(61), HCNC Tring(10)
31	-	-	1136.33	1090.877	0.0023	1.5162	HCNC Tring(61) bHCH(21) HCNC Tring(10)
32	-	-	1129.0	1083.84	209.9245	115.6805	NC _{ss} (13), bHCC(16) bHCC(12)
33	1068.76	-	1079.51	1036.33	26.3086	1.1454	HCNC Tring(54), NC _{ss} (24), bHCH(15)
34	-	-	1014.41	973.8336	6.5158	0.1541	bCCC(70), bCCC(10),
35	996.41	-	982.25	942.96	0.0000	0.0473	HCNC Tring(72),
36	968.06	-	974.84	935.8464	2.9108	6.8779	HCNC Tring(65),
37	940.13	-	959.23	920.8608	19.9994	52.6601	CC _{ss} (63),HCNC Tring(10)
38	-	-	868.32	833.5872	16.7679	0.0029	NC _{ss} (14),CC _{ss} (10) bONO(49)
39	-	-	835.16	801.7536	53.3425	0.1927	HCCC Tring(76)
40	-	-	806.74	774.4704	0.0001	7.5478	HCCC Tring(95)
41	749.91	749.11	762.64	732.1344	7.8729	1.1360	CC _{ss} (37)bONO(16) bCCC(31)
42	-	-	737.65	708.144	9.5305	0.0211	Out of planeOCON(88)
43	696.19	-	700.93	672.8928	15.0804	5.5670	CCCC Tring(10) CCCC Tring(62)
44	628.64	640.54	644.54	618.7584	0.6701	3.3584	bCCC(74) bCCC(10)
45	605.03	-	616.93	592.2528	4.2180	3.3879	bCCC(17) bCCC(14) bONO(14))CC _{ss} (15),
46	540.31	-	547.82	525.9072	5.5578	0.5704	bCNC(69) CC _{ss} (15)
47	505.16	-	497.12	477.2352	10.7935	0.220	CCCC Tring(70) HCCC Tring(11) CCCC Tring(10)
48	490.73	-	476.26	457.2096	2.1044	5.6947	bCNC(61)
49	-	-	471.19	452.3424	0.0054	0.0215	NC _{ss} (11) bCCC(69)
50	-	-	432.76	415.4496	0.0000	0.1854	CCCCTring(51)
51	-	-	310.33	297.9168	0.5019	5.1515	CCCC Tring(22) CCCC Tring(11)
52	-	-	303.54	291.3984	0.0068	2.0231	CCCC Tring(70) CCCC Tring(12)
53	-	-	287.94	276.4224	0.1731	1.6475	bCCC(31) bCCC(14) NC _{ss} (19) CC _{ss} (21)
54	-	-	197.50	189.6	4.3097	0.2017	bCNC(86)
55	-	-	184.16	176.7936	0.0143	0.0121	Out of planeCCCN(66)
56	-	-	173.82	166.8672	0.5200	0.9086	HCNC Tring(64) CCNO Tring(17)
57	-	-	79.46	76.2816	0.0012	0.4327	bCNC(84)
58	-	-	78.87	75.7152	0.6387	0.4524	CCNO Tring(78) HCNC Tring(10)
59	-	-	57.32	55.0272	0.0000	1.4330	CCCC Tring(49) CCCC Tring(17)
60	-	-	16.12	15.4752	1.4047	0.6528	CCNO Tring(87)
							HCNC Tring(69)

Abbreviations used; b-bending, T-torsion, ss-symmetric stretching

Optical Studies

UV-Vis-NIR Analysis

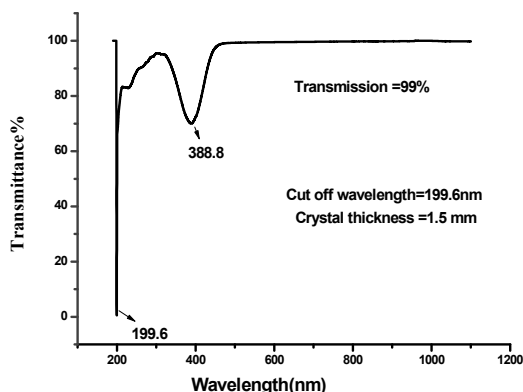


Fig 5 Optical transmission of DMNA

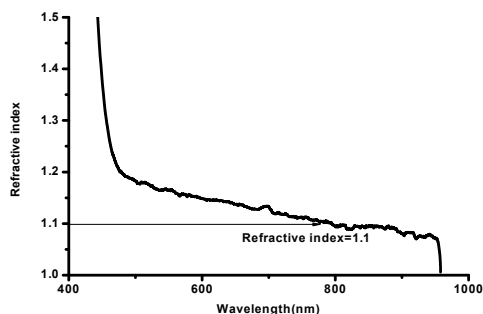


Fig 6 Plot between refractive index vs wavelength

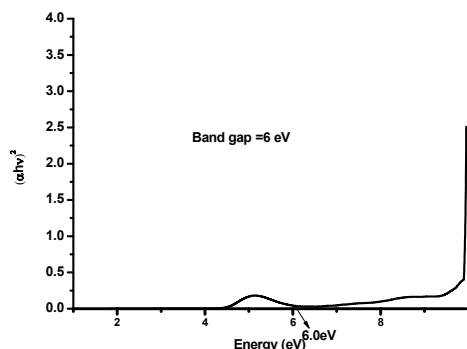


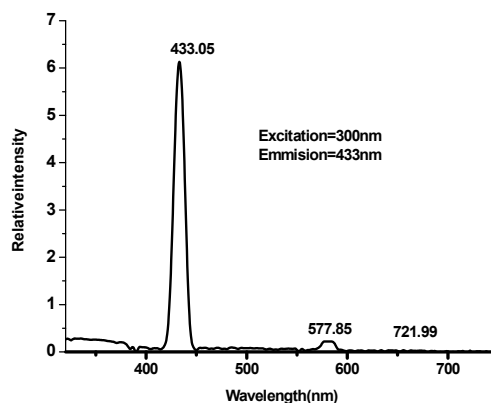
Fig 7 plot between energy vs $(\alpha h\nu)^2$

The UV-Vis-NIR spectrum of DMNA has been recorded in the region between 200-1100nm by using Perkin Elmer lamda 35 spectrophotometer is shown in Fig. 3. The crystal has wider transparency in the visible and NIR region. The lower cut-off wavelength is observed at 199.6 nm. This low value of lower cut-off wavelength and higher transmission is well suited for frequency conversion of 1064nm laser radiation. The variation of $(\alpha h\nu)^2$ versus incident photon energy $(h\nu)$ relation in the fundamental absorption region is plotted in Fig. 3.2. The optical energy band gap of the crystal is found be 6.0 eV. The plot between refractive index and wavelength is shown in Fig. 6. From the graph refractive index decreases with increasing wavelength [24]. The obtained refractive index value of the DMNA crystal is 1.1 for the wavelength determined from the graph is 1.1 at 800nm. The absence of absorption band in the visible region and the wide band gap of the grown crystal

attest its suitability of the grown crystal for photonic and optical applications [25]

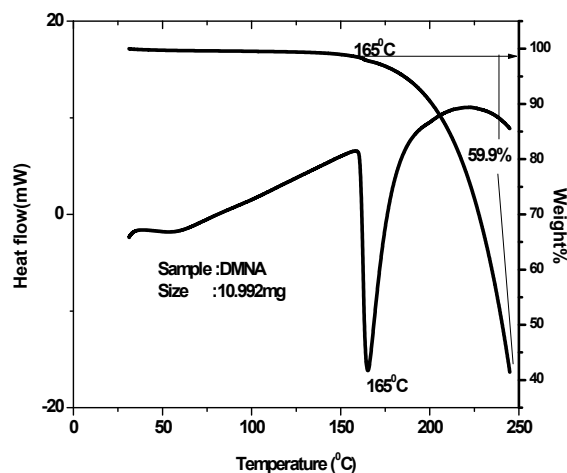
Photoluminescence

The Photoluminescence study was recorded by using the Perkin Elmer LS45 Spectrofluoro meter in the range from 300 -800 nm in Fig. The given sample was excited as 400nm [26]. The sharp emission peak is observed from the emission spectrum is at 433nm. This shows that the grown crystal has blue emission property. The strong emission peak indicates the presence of intrinsic effects in the forbidden gap region. The grown crystal emission region is visible which reveals the material is suitable for optical applications [27].



TGDTA Analysis

The TGA/DTA analysis were carried out by STDQ 600 thermal analyser at a heating rate of 10^0 K /min in Nitrogen atmosphere. The Decomposition of DMNA begins at 165^0 C. It shows that the grown crystal thermally stable upto 165^0 C. The endothermic peak observed in DTA at 165^0 C. The sharp endothermic peak observed in DTA shows good crystalline nature of the above materials. The one stage decomposition observed in TGA, the sample losses its weight by 60%. The high melting point and good thermal stability is much more suitable for device fabrication [28].



SHG measurements

The SHG efficiency of the grown crystals has been carried out by Kurtz and Perry technique using Nd-YAG laser with 1064nm radiation. The laser energy incident on the densely packed capillary tube was chosen as input pulse energy

1.2mJ/sec and pulse width 10 ns. The second harmonic generation was confirmed by the emission of green radiation (532nm). The same input energy is used for the sample KDP and Urea. The SHG relative efficiency of the grown crystal (210mV) has been observed to be nearly 9 times greater than that of KDP (24mV) reference sample [29].

CONCLUSION

The good NLO crystal of DMNA were grown by the slow evaporation solution growth method by using the mixture of methanol as a solvent. The crystal structure of the grown crystal is elevated from the single crystal XRD. The optical transparency of the grown crystal is determined by the UV-Vis analysis and also the optical behaviour of the grown crystal was found by using Photoluminescence study. TGDTA analysis is confirmed that the crystal has good thermal stability below to 150°C. The theoretical hyperpolarisability calculation express the suitability of the grown crystal for the fabrication of opto electronic devices. The grown DMNA crystal is found to have good NLO property compared to KDP (is 9 times greater than KDP).

Acknowledgements

The authors are thankful to Dr.P.K .Das, IISc, Bangalore for SHG measurements and also Pondicherry University for TGDTA analysis.

References

1. A.Dulcic, C.Sauteret, The regularities observed in the second order hyperpolarizabilities of variously disubstituted benzenes, *The Journal of Chemical Physics* 69, 3453 (1978).
2. J.F. Nicoud, R.J. Twieg, D.S. Chemla, J.Zyss(Eds), *Nonlinear optical Properties of Organic Molecules and Crystals, Vol.1*, Academic Press, New York, 1987, chapter II-III,pp.277.
3. M.Jalali-Heravi, A.A.Khandar, I. Shei Kshoae, Characterization and theoretical investigation of the electronic properties and second-order nonlinearity of some three dentate salicylaldiminato Schiff base ligands, *Spectrochim. Acta Part A*2000, 56, 1575.
4. H.S. Nalwa, T. Watanabe, S. Miyata, *Nonlinear optics of Organic Molecules and Polymers*, CRC Press, Bota Raton,FL,1997
5. M.G.Kuzyk, C.W.Dirk (Eds.), *Characterization Techniques and Tabulations for Organic Nonlinear optical Materials*, Marcel Dekker, Inc, New York,1998.
6. J.L.Oudar, J.Zyss, Structural dependence of nonlinear-optical properties of methyl-(2,4-dinitrophenyl)-aminopropanoate crystals, *Phys. Rev. A* 26(1982)2016
7. J.Zyss, J.L. Oudar, Relations between microscopic and macroscopic lowest-order optical nonlinearities of molecular crystals with one- or two-dimensional units, *Phys. Rev. A* 26(1982)2028
8. O.Y. Borbulevych, Ronald.D. Clark, Experimental and theoretical study of N,N Dimethyl 4-Nitroaniline derivatives as model compound of Non-linear optical organic materials, *J. Molecular Structure* 604(2002)73-86.
9. Frisch MJ, Trucks GW, Schlegel HB, Scuseria GE, Robb MA (2010) *Gaussian, Inc.*, Wallingford CT.
10. Mukherjee V, Singh NP, Yadav RA (2011) Optimized geometry and vibrational spectra and NBO analysis of solid state 2,4,6-tri-fluorobenzoic acid hydrogenbonded dimer. *J Mol Struct* 988: 24-34.
11. Glendening ED, Reed AE, Carpenter JE, Weinhold F (1998) NBO Version 3.1, TCI, University of Wisconsin, Madison.
12. N.Prabhavathi, N.Senthil Nayaki, V.Krishnakumar, Spectroscopic Investigation (FT-IR, FT-Raman, NMR and UV-Vis), Conformational Stability, NBO and Thermodynamic Analysis of 1-(2-Methoxyphenyl) Piperazine and 1-(2-Chlorophenyl) Piperazine by DFT Approach *Pharm Anal Acta* 6(2015)2153-2435
13. Kleinman DA (1962) Nonlinear Dielectric Polarization in Optical Media. *Phys Rev* 126: 1977-1979.
14. Prabavathi N, Nilufer A, Krishnakumar V (2012) Molecular structure, vibrational, UV, NMR, hyperpolarizability, NBO and HOMO-LUMO analysis of Pteridine2,4-dione. *Spectrochim Acta A* 99 (2012) 292-302.
15. Reed AE, Curtiss LA, Weinhold F (1988) Intermolecular interactions from a natural bond orbital, donor-acceptor viewpoint. *Chem Rev* 88: 899-926.
16. Foster JP, Weinhold F (1980) Natural hybrid orbitals. *J Am Chem Soc* 102: 7211-7218.
17. Rajith L, Jissy AK, Girish Kumar K, Datta A (2011) Mechanistic Study for the Facile Oxidation of Trimethoprim on a Manganese Porphyrin Incorporated Glassy Carbon Electrode. *J Phys Chem C* 115: 21858-21864.
18. Sebastian S, Sundaraganesan N (2010) The spectroscopic (FT-IR, FT-IR, gas phase, FT-Raman and UV) and NBO analysis of 4-Hydroxypiperidine by density functional method. *Spectrochim Acta Part A* 75: 941-952.
19. G.Varsanyi, Assignment for vibrational spectra of seven hundred benzene derivatives, Vol,1-2,Academic Kiaclo, Budapest,1973.
20. J. Mohan, organic spectroscopy, Principles and applications, second ed., New age international (P)Limited Publishers, New Delhi,2001
21. M. Karabacak, C. Mehmet, Z.Una, M. Kurt, FT-IR, UV spectroscopic and DFT quantum chemical study on the molecular conformation, vibrational and electronic transitions of 2-aminoterephthalic acid, *J. Mol. Struc.* 982 (2010) 22.
22. Robert M. Silverstein, Francis X.Webster, David J.Kiemle, *Spectrometric identification of organic compounds*, Seventh edition, John willey & sons. Inc., United state of America, 102-104 (2005).
23. K.Sangeetha, L. Guruprasad, R.Mathammal, Crystal growth, vibrational, optical, thermal and theoretical studies of a nonlinear optical material: 2-Methyl 3,5-dinitrobenzoic acid, *Physica B* 501(2016)5-17
24. G. Bhuvaneswari, L. Guru Prasad, N. Prabhavathi, Structural, optical, thermal and theoretical investigations on high efficiency NLO crystal: 4-Nitrobenzonitrile, *Optik* 157 (2018) 1078-1086
25. Sheikshoae, S. Saeid-Nia, N. Monadi, H. Khabazzadeh, Some Quantum chemical study about the Second order Non-linearity of Two-imino Chromophores containing salen group, *J. Appl. Phys.* 7 (2007) 145.
26. V. Krishnakumar, L. Guru Prasad, and R. Nagalakshmi Investigation on 3-aminophenol a nonlinear optical

- crystal for frequency doubling, *Eur. Phys. J. Appl. Phys.* 48, 20403 (2009).
27. Narayan Bhat M, Dharmaprakash SM, Effect of solvents on the growth morphology and physical characteristics of nonlinear optical g-glycine crystals, *J.Crystal growth* 2002;242;245-252
28. V.Krishnakumar, L.Guruprasad, R.Nagalakshmi, P.Muthusamy, Physicochemical properties of organic nonlinear optical crystal for frequency doubling: Glycine acetamide, *Material letters*,63(2009)1255-1257
29. Kurtz S.K and Perry T.T (1968) a Powder technique for the evaluation of NLO Materials, *Journal of Applied physics*, 39, 3798 -3813.

How to cite this article:

Bhuvaneswari G., Prabavathi N and Guru Prasad L (2018) 'Crystal Growth, Experimental, and Theoretical Investigation of Organic Nlo Material N, N Dimethyl -4 Nitro Aniline', *International Journal of Current Advanced Research*, 07(12), pp. 16442-16448. DOI: <http://dx.doi.org/10.24327/ijcar.2018.16448.3040>
